Proceedings of the
Annual Stability Conference
Structural Stability Research Council
Louisville, Kentucky, April 13-16, 2021

Steel plates in combined shear and moment: flat versus LFS profiles

Peter Y. Wang[1], Parfait M. Masungi [2], Maria E.M. Garlock[3], Spencer E. Quiel[4]

Abstract
Slender steel plates are susceptible to shear buckling in nearly all of their myriad applications, including plate girders. Traditional strategies to enhance web shear buckling strength include welded stiffeners and corrugated webs, but these are subject to higher fatigue sensitivity and specialized fabrication requirements, respectively. The authors propose a novel strategy, introducing low-frequency sinusoids (LFS) in the web along its length. The LFS have been shown to increase web shear buckling strength substantially with minimal increase in material and greater fabricability. However, their combined shear and moment capacity have yet to be studied. This paper studies various combinations of pure shear, high shear – low moment, pure moment, and high shear – high moment. Experimentally validated finite element analyses are used to determine elastic shear buckling loads and ultimate loads as well as web stress distributions. Results show that LFS have slightly greater moment strength than corrugated webs but less than flat webs; they are thus suitable for high-shear low-moment situations, though additional flange reinforcement may be needed for high-shear high-moment situations.

1. Introduction
The design, mechanics, and behavior of welded steel I-shaped plate girders have been studied for more than half a century. The main purpose of the top and bottom flanges is to resist bending moment by developing an axial tensile and compressive force couple originating from the bending action, and the main web function is to resist shear forces (Graciano and Ayestarán 2013). In the early 1960s, researchers extensively studied the strength of welded plate girders by conducting experimental tests under predominant shear as well as combined shear and bending moment to evaluate the strength and behavior based on classical beam theory established by Navier and St. Venant (Basler et al. 1960; Basler 1961; Basler and Thurlimann 1961). Immediately following these early studies, many researchers have focused on studying the behavior and mechanics of plate girders subject to pure shear or pure bending moment but rarely in combination. However, most structures experience both shear and moment. Prior to the year 2000, most design specifications (AISC 1999; AASHTO 1998) considered the interaction of moment and shear only when large moment was present. Interaction equations derived by Basler were later discarded in updates to these specifications (AASHTO 2004; AISC 2005) based on the work conducted by

[1] PhD Candidate, Princeton University, <pywang@princeton.edu>
[2] PhD Candidate, Princeton University, <pmasungi@princeton.edu>
[3] Professor, Princeton University, <mgarlock@princeton.edu>
[4] Associate Professor, Lehigh University, <seq213@lehigh.edu>

White et al. (2004) which demonstrated that the equations of these specifications sufficiently capture the resistance of a comprehensive body of experimental test results without the need to consider shear and bending moment interaction.

Work done by Lee et al. (2013) demonstrated that there is complexity in the behavior of plate girders subject to combined shear and bending moment. The presence of shear forces and bending moments on plate girders automatically establishes an interaction relationship – for example, a web that reaches its capacity in shear cannot simultaneously reach the bending moment capacity. Azizinamini et al. (2007) conducted experimental tests of doubly symmetric plate girders subjected to combined high shear and high bending moment and observed that the significance of the shear and moment interaction was minor. Lee et al. (2013) mentioned that there can only be three approaches to reflect the shear and bending interactions: (1) reducing the shear strength, and keeping the full bending moment strength; (2) reducing the bending moment strength and keeping the full shear strength; and (3) simultaneously adjusting both the shear and bending moment strength (Lee et al. 2013). In practice, adjusting both the shear and bending moment is undesirable by designers due to the complexity. Adjusting the shear strength is simpler than adjusting the bending moment strength because it can be done by simply adjusting the spacing of intermediate transverse stiffeners. In contrast, adjusting the bending moment strength necessities a change in the whole cross section. White and Barker (2008) pointed out that even though the consideration of shear and bending moment is important for theoretical contributions, it implies a level of precision that cannot be achieved; hence, regardless of the type of analytical approaches and considerations which involve idealization of the physical response, refinement would only complicate the design and is not expected to lead to any significant improvement.

In terms of shear behavior, the strength of slender plates is dependent on the thickness, imperfections, material properties, and aspect ratio *a/D* (where "*a"* represents the space between vertical stiffeners and "*D"* represents the depth of web). The ultimate shear strength of a thin plate, V_u, can be defined by the sum of the elastic shear buckling load, V_{cr} and a postbuckling reserve (Timoshenko 1961; Lee et al. 1996). In slender plates, these buckling limit states are typically reached well before the plastic shear capacity, V_p. Design methods to increase V_{cr} and V_u such as the addition of welded transverse (vertical) or longitudinal (horizontal) stiffeners to restrain out-of-plane displacement have presented an array of practical concerns such as fatigue sensitivity and labor and material cost (Balaji Rao et al. 2013; Škaloud et al. 2013). To avoid using transverse stiffeners, alternatives such as corrugated web plates (as shown in Fig. 1(a) with corrugations in the direction of the girder span) may be used with triangular (zig-zag), trapezoidal, or sinusoidal shape in the longitudinal direction (Riahi et al. 2018). The literature indicates that though corrugated plates can augment the shear behavior, they require highly specialized equipment and fabrication processes (Pasternak and Kubieniec 2010; Siokola 1997) when forming and assembling the plates.

As an alternative to transverse stiffeners or corrugated plates, the authors have introduced low-frequency sinusoidal (LFS) plates as a means to enhance the shear capacity as shown in Fig. 1 (Wang et al. 2021). While the authors have studied the response of these plates under pure shear load, this paper presents for the first time an evaluation of LFS plates under combinations of high shear and high moment, high shear and low moment, and pure moment. Experimentally validated

finite element (FE) modeling techniques were used to make comparisons and evaluations on the effect of moment on LFS plates.

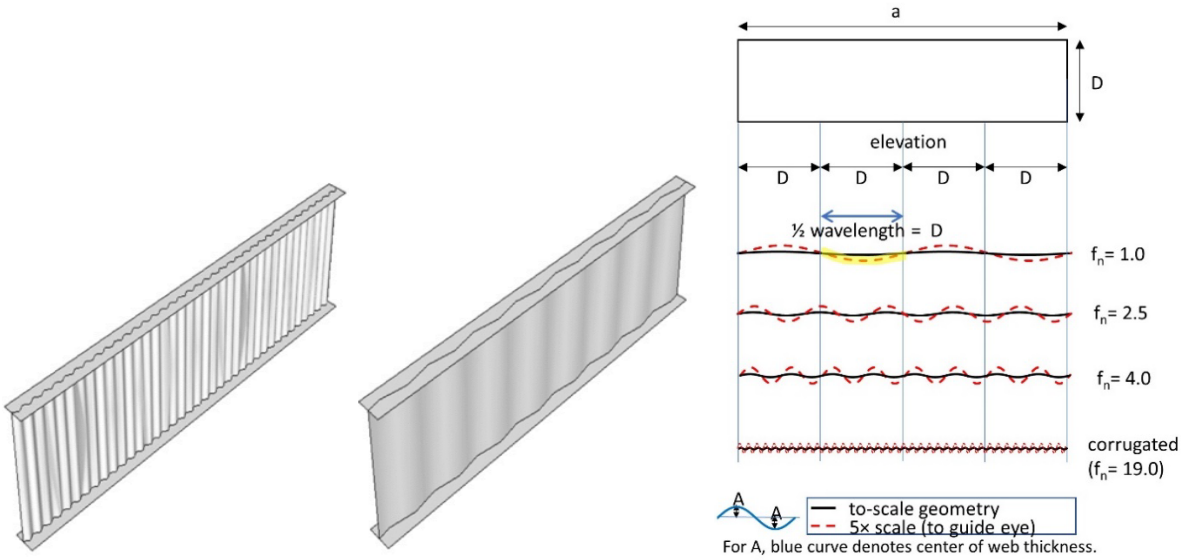

(a) corrugated (b) LFS (c) LFS parameters

Figure 1: Representation of plate girders with: (a) typical corrugated web and (b) low-frequency sinusoidal (LFS) web, and (c) LFS geometry defining normalized wave frequencies (f_n), and an amplitude (A).

2. LFS Plate Girders Subject to Pure Shear

Recent work by the authors (Wang, et al. 2021) proposed a constructible and potentially fatigue-resistant alternative to increase the shear buckling strength of thin steel plates by introducing low-frequency sinusoids (LFS) with frequencies lower than those used in commercial corrugated web plates (Pasternak and Kubieniec 2010). "Low-frequency" characterizes sinusoids with a full wavelength on the order of 0.7 m or longer, where the shortest wavelength is associated with the highest frequency (e.g. $f_n = 4$ in Fig. 1). Parametric variations of the LFS plates can include the amplitude (A), the magnitude of the initial imperfections, and the normalized wave frequency (f_n). The variable f_n refers to the number of half waves in the distance equal to the depth of the web (D) (see Fig. 1(c)). An f_n value of 0 indicates that the geometry of the web plate is completely flat (except for initial imperfections). The amplitude (A) is the transverse distance from flange centerline to the centerline of the web at the peak of the sinusoid.

Using validated FE models, the authors studied LFS plate girders under pure shear loading while varying the LFS design parameters (f_n, A), initial imperfection (out-of-flatness) of the LFS web plate, and the web plate depth and slenderness (depth/thickness) (Wang et al. 2021). The results showed that substantial increases in shear strength could be achieved using LFS webs, with the following specific enhancements: (a) the ultimate shear capacity increased up to 87% over flat webs; (b) V_{cr} was found to increase significantly with f_n; and (c) for f_n values greater than 1.5, an inelastic limit state such as V_u (sometimes nearly equaling the plastic shear strength V_p) is reached before V_{cr} is achieved. Also, given a similar quantity of material, a much larger increase in shear capacity is possible by increasing wave frequency f_n than by increasing amplitude A.

When compared to corrugated webs, Wang et al. (2021) found that "efficiencies" equal to or greater than typical corrugated webs can be achieved using LFS, where a measure of "good"

efficiency equals V_u / V_p ratios of 0.8 or larger (Sayed-Ahmed 1998). Further, the length of steel required to fabricate LFS web plates with A = 3 cm and f_n ranging from 1 to 4 is only up to 2% more than a flat plate and 13% less than a corrugated plate, assuming the same plate thickness.

Thus, LFS plates lead to an increase in shear strength with negligible increase in material quantities. Additional notable advantages to this LFS strategy include: (1) a simple fabrication process (Wang et al. 2020) and (2) the elimination of the need to use welded stiffeners thus reducing fatigue sensitivity and weight. Despite the economic and shear performance advantages, the previous work by the authors recognized that LFS webs will reduce the plastic moment capacity of the section. LFS designs are thus most efficient in locations with high shear and low moment. Otherwise, the LFS flexural strength can be enhanced with larger flange plates and/or higher flange yield stress material. A numerical study of the effects of moment on the capacity of LFS plates is therefore the focus of this paper.

3. Parameters of Study

3.1 Span, Structure, and Loading

The span, structure type, and loading conditions are parametrically evaluated for both flat and LFS plates using finite element (FE) analysis. Four types of structures were evaluated with the appropriate boundary conditions: (1) a cantilever panel (*CP*) under a concentrated and uniformly distributed loads as shown in Fig. 2(a); (2) a moment panel (*MP*) under bending moment action as shown in Fig. 2(b); (3) a full beam (*FB*) with a point load applied at midspan as shown in Fig. 2(c); and (4) a pure shear loaded panel (*SP*) as shown in Fig. 2(d). In the case of concentrated load for *CP*, a shear edge load $P = qD$ was applied in the upward direction on the vertical edge of the web plate (see Fig. 2(a)). For distributed loading in the *CP* case, a uniform load was applied vertically downward and distributed across the whole area of the top flange (see Fig. 2(a)). For the moment loading condition in the *MP* case, coupled moments were applied on each web end at the mid-depth of the web (see Fig. 2(b)). The span of the structure as it relates to the aspect ratio (a/D) considered both short and long spans so that conditions of high shear and high/small moment can be achieved. For a short span structure (high shear - small moment), an aspect ratio of a/D = 2 is utilized. For a long span structure (high shear - high moment) an aspect ratio of a/D = 4 is utilized.

	U_x	U_y	U_z	UR_x	UR_y	UR_z
Edges ①	*X*	*X*	*X*	*X*	*X*	*X*
Edge ②			*X*			

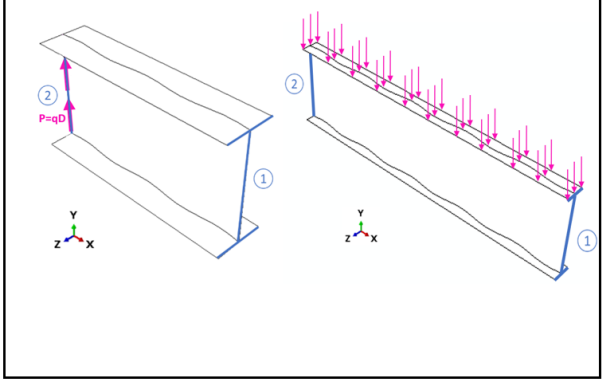

(a) Cantilever Panel (*CP*)

	U_x	U_y	U_z	UR_x	UR_y	UR_z
Point ●		*X*	*X*	*X*		
Point ●			*X*	*X*	*X*	*X*
End Cross section ①	Kinematically constrained to its Point ●					
Edge ②	*X*					

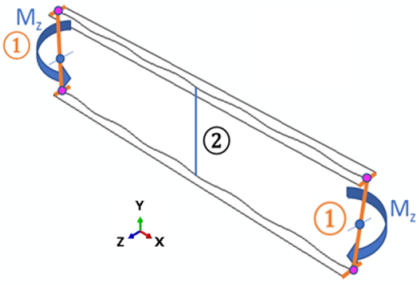

(b) Moment Panel (*MP*)

	U_x	U_y	U_z	UR_x	UR_y	UR_z
Line	*X*	*X*				
Line		*X*				
Line	Downward applied load					
Point			*X*			

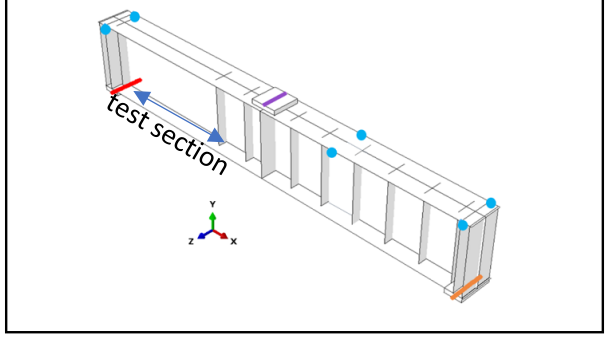

(c) Full beam (*FB*)

	U_x	U_y	U_z	UR_x	UR_y	UR_z
Edge ①	*X*		*X*	*X*		*X*
Point	*X*	*X*	*X*	*X*	*X*	*X*
Point	*X*			*X*	*X*	*X*

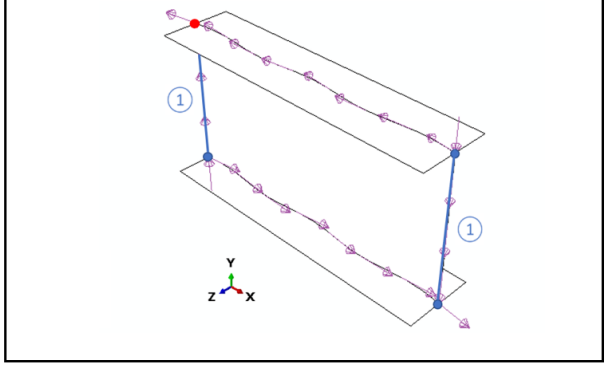

(d) Pure Shear Panel (*SP*)

Figure 2. Structure, loading cases, and conditions.

3.2 Prototypes

The girder prototypes shown in Table 1 are based on (1) the FHWA 2012 design example for a 3-span continuous bridge (Grubb and Schmidt 2012) and (2) the FHWA 1982 *Standard Plans for Highway Bridges* (FHWA 1982). These two prototypes have been used in different studies by the authors with similar scale and slenderness. While the flanges of the FHWA 2012 design example used steel with a yield stress F_y =70 ksi (483 MPa), which is higher than the web and stiffeners, the modeled girders use one F_y value throughout for simplicity as listed in Table 1. The FHWA2012-b model represents the finalized prototype used in the experimental program by the authors (Wang et al. 2020), and thus the yield stress accounts for the expected yield instead of nominal yield. This prototype is used to study high shear and low moment in Set 2 of Table 2. Both FHWA2012-a and FHWA-b prototypes were modified with larger flange widths to account for not using higher strength steel and to add safety factor to avoid lateral torsional buckling failure.

The moment capacity of a fully yielded cross section is defined by the plastic moment (M_p) per Eq. 1, where Z is the plastic section modulus. The flange moment (M_f) is characterized by the moment carried by the flanges alone when the stresses over the flange cross section equal the yield stress and is calculated using Eq. 2, where H is the distance between the centerline of the flanges and A_f is the area of one flange. The plastic shear capacity, V_p, is a function of the web area, A_w, as shown in Eq. 3. These values are calculated for each prototype in Table 1 and used later to compare with the FE results.

$$M_p = F_y Z \tag{1}$$

$$M_f = F_y H A_f \tag{2}$$

$$V_p = \frac{1}{\sqrt{3}} F_y A_w \tag{3}$$

Table 1: Girder Prototypes

Prototype	D in (m)	t_w in (mm)	D/t_w	t_f in (mm)	b_f in (m)	F_y ksi (MPa)	M_p k-ft (kN-m)	M_f k-ft (kN-m)	V_p k (kN)
FHWA2012-a	69 (1.75)	0.50 (13)	138	1.375 (35)	24 (0.61)	50 (345)	12,156 (16,582)	9,677 (13,148)	996 (4,430)
FHWA2012-b	69 (1.75)	0.50 (13)	138	1.375 (35)	33 (0.84)	55 (378)	17,363 (23,542)	14,636 (19,844)	1,096 (4,873)
FHWA1982	58 (1.47)	0.44 (11)	133	1.063 (27)	14 (0.36)	50 (345)	5,204 (7,070)	3,662 (5,020)	737 (3,278)

3.3 Parametric Study Matrix

The parametric study matrix is shown in Table 2 and summarizes the loading cases, structure types (*CP, MP, SP* and *FB*), the aspect ratio, the girder type (Flat or LFS), and the prototype (per Table 1). Frequencies ranging from 0 to 3 in the case of shear and moment interaction were considered. In the case of the *CP* and *MP* structure for the LFS girder, frequencies of 2.5 and 4 were used to demonstrate an increase in the shear carrying capacity (Wang et al 2021). The implications of this study matrix provide a robust comparison of flat versus LFS plate girder behavior under shear only, high shear and low moment, high shear and high moment, and moment only.

Table 2: Parametric Study Matrix

Set	Description (1)	Loading	Structure (2)	a/D	Type	Wave Parameters(3)		Prototype
						f_n	A in. (cm)	
1	Valid.	V+M (point)	CP	2	LFS	2, 2.5, 3	1.18 (3)	FHWA2012-a
1	Valid.	V+M (exp.)	FB	2	LFS	0.5 → 3	1.18 (3)	FHWA2012-a
1	Valid.	V+M (exp.)	FB	2	Flat	0	0	FHWA2012-a
2a	V	V only	SP	2	Flat	0	0	FHWA2012-b
2a	V	V only	SP	2	LFS	0.5 → 3	1.18 (3)	FHWA2012-b
2b	hV-sM	V+M (point)	CP	2	Flat	0	0	FHWA2012-b
2b	hV-sM	V+M (point)	CP	2	LFS	0.5 → 3	1.18 (3)	FHWA2012-b
3a	M	M only	MP	4	Flat	0	0	FHWA1982
3a	M	M only	MP	4	LFS	2.5, 4	1.18 (3)	FHWA1982
3a	M	M only	MP	4	Corr.	19	0.8 (2)	FHWA1982
3b	hV-hM	V+M (point)	CP	4	Flat	0	0	FHWA1982
3b	hV-hM	V+M (point)	CP	4	LFS	2.5	1.18 (3)	FHWA1982
3b	hV-hM	V+M (point)	CP	4	Corr.	19	0.8 (2)	FHWA1982
3b-u	hV-hM	V+M (unif.)	CP	4	Flat	0	0	FHWA1982
3b-u	hV-hM	V+M (unif.)	CP	4	LFS	2.5	1.18 (3)	FHWA1982
3b-u	hV-hM	V+M (unif.)	CP	4	Corr.	19	0.8 (2)	FHWA1982

(1) Description: **Valid.** = validation study; **V** = shear only; **hV-sM** = high (large) shear (V) and small moment (M); **hV-hM** = high shear (V) and high moment (M); **M** = moment only. (2) structure: cantilever panel (**CP**), full beam (**FB**), moment panel (**MP**), or shear panel (**SP**). (3) LFS specimen with frequency f_n and amplitude A **(**cm**)** will be identified as F[f_n]-A[A]**.**

4. Finite Element (FE) Model and Panel Validation Study

To investigate the shear and moment interaction of flat and LFS plates, this study utilizes a nonlinear FE approach in ABAQUS 2017 that was developed and experimentally validated in the

authors' previous work (Wang et al. 2021). LFS models neglected residual stresses that would result from fabrication or forming. Four-node "S4" shell elements ("doubly-curved, finite membrane strains, general purpose") were used (Dassault Systemes 2017) with a roughly 5-cm mesh dimension (see Fig. 3), as determined by a convergence study on the elastic buckling load of a flat web panel (Wang et al 2019). Young's modulus of E=200 GPa, Poisson's ratio equal to 0.3, and yield stress F_y specified in Table 1 were employed. The stress-strain curve is elastoplastic with strain-hardening per Eurocode 3, Part 1-2 (CEN 2001).

An elastic eigenvalue analysis was used to determine V_{cr} of each girder specimen. For the subsequent nonlinear analyses, a scaled initial geometric imperfection of the first buckled eigenmode was imposed on the web plate to allow bifurcation and represent realistic geometric imperfections in the field. A nonlinear Modified Riks analysis was used to determine V_u of each loaded specimen (Glassman and Garlock 2016). Typical imperfection magnitudes in practice can range between D/100 to D/1000 (Gomez 2020; Driver et al. 2006), and the current study therefore employs D/1000. The effect of imperfections on the pure shear capacity of LFS is discussed by the authors based on initial geometric imperfections of D/10,000, D/1000, D/400 and D/100 in their previous work (Wang et al. 2021).

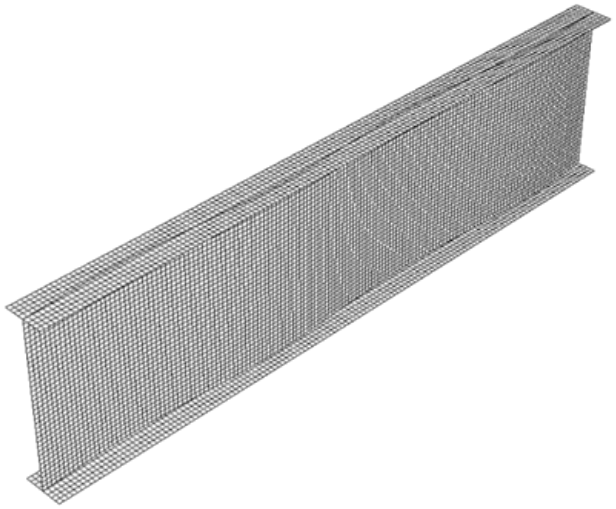

Figure 3: Finite element mesh

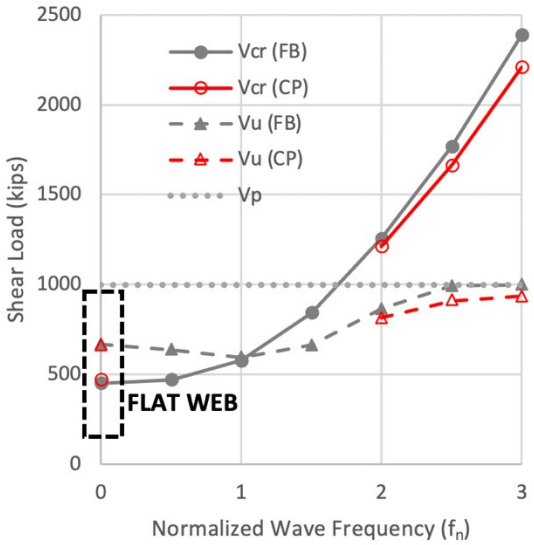

Figure 4. Validation of *CP* model by comparison of V_{cr} and V_u to *FB* model (for flat web and various f_n– see Fig. 1(c).)

As an initial demonstration, the cantilever panel model (*CP*) is compared against the full beam model (*FB*) using the FHWA2012-a specimen (Set 1 of Table 2). The *CP* panel model and the test section of the *FB* model have identical shear and moment diagrams and would be expected to show similar shear buckling behavior. Fig. 4 presents a comparison of these two models for the flat web (f_n = 0) and other various f_n values. V_{cr} and V_u and V_p are plotted, where V_p is constant for all f_n as defined by Eq. 3. Fig. 4 shows that the *CP* and *FB* results are nearly identical for the flat web models. The results for f_n equal to 2, 2.5, and 4 show that the *CP* and *FB* results follow the same trends, and V_u does not exceed V_p. The *CP* model results are slightly smaller than the *FB* results since the *FB* model has plates that extend beyond the test section as seen in Fig. 2(c). However, the *CP* model provides adequate and conservative results for the subsequent studies presented in

this paper. Fig. 4 also shows the relationship between LFS parameters and shear strength and follows the same trend as that published by Wang et al. (2021) and summarized in Section 2. The influence of small moment on shear capacity will be discussed in detail next using *CP* models.

5. Short Span: High Shear, Small Moment

In this section, model Set 2a and 2b, as shown in Table 2, are used to evaluate the effects of moment on a short span (a/D = 2), which results in high shear (hV) and small moment (sM) on the *CP* model. For this evaluation, the FHWA2012-b prototype is used (see Table 1). Fig. 5 shows that the flat web model with pure shear loading (blue lines) has similar V_{cr} and V_u values compared to the combined moment and shear loading (red lines). The V_{cr} values are not affected by the addition of moment for all f_n values since the lowest eigenvalue remains to be a shear mode. Similarly, the addition of small moment does not impact the ultimate strength of the LFS webs for the f_n values presented. Both the shear only and the combined moment and shear model capacities are capped by V_p at large f_n values. Hence, economic advantages are possible by using LFS webs for shear and flexural strength gain when shear dominates and small moments develop on a structure.

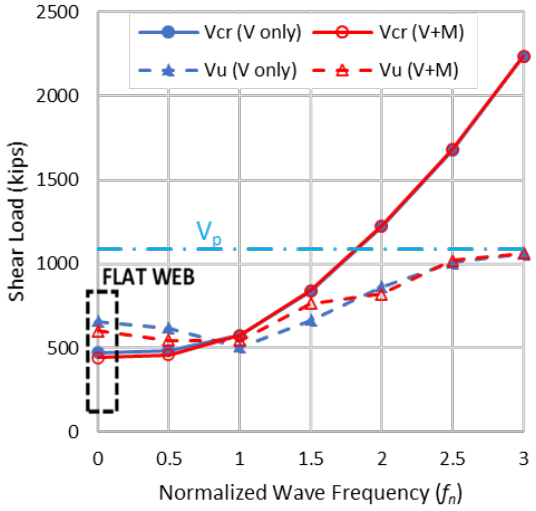

Figure 5. Effects of moment for Set 2a and 2b (see Table 2), for a/D = 2 panel representing high shear – low moment, loaded in pure shear (V only) and combined shear and moment (V+M).

6. Longer Span: High Shear, High Moment

This section evaluates the effect of moment using Set 3 of Table 2. The FHWA1982 prototype is used for this evaluation (see Table 1). Set 3a is loaded with moment only (a/D = 4) for a direct evaluation of the flexural capacity of LFS plates compared to flat plates. Set 3b uses the *CP* model to examine a high shear and high moment loading condition via a/D = 4 with a point load. In addition, Set 3b-u is the same as Set 3b, except that the loading condition is a uniform load that causes the same shear at the support and thus a different ratio of moment-to-shear as seen in Fig. 6. The different loading scenarios can also represent live load and dead load scenarios.

As shown in Fig. 2, the longitudinal ends of the specimens are assumed to be laterally braced, so the effects of lateral torsional buckling are eliminated for this study. Though not shown here, the girder's lateral torsional buckling load is shown to increase with LFS, similar to how it does for corrugated webs. A full study of lateral torsional buckling is beyond the scope of this paper.

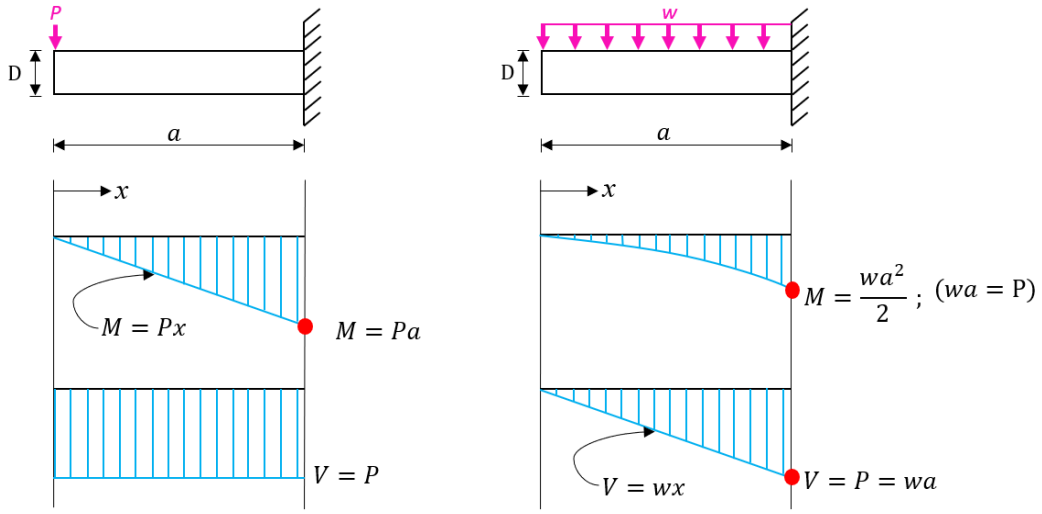

Figure 6. *CP* model with (a) point load – Set 3b and (b) uniformly distributed load – Set 3b-u (see Table 2)

Fig. 7 plots the normal stresses in the web only (at the ultimate moment) using the pure moment loading of Set 3a. The flat web reaches yield (345 MPa) over more than half of its depth, demonstrating the web's participation in resisting moment-induced stress. In contrast, neither the LFS web specimens nor the corrugated web specimen reach yield anywhere in the web. Due to the 'accordion effect' (i.e. a reduced axial stiffness in corrugated webs (Abbas et al. 2006)), the corrugated web is observed to have near zero web normal stress for a vast majority of the web (except at the top and bottom of the web where it interfaces with the flanges). This agrees well with the Eurocode equation for determining moment capacity of the corrugated web (CEN 2006), which assumes a "flanges only" moment capacity calculation that neglects all contribution of the web to the moment strength (M_f). The bending stress distributions of the LFS webs fall between these bounds corresponding to a flat and corrugated web. An LFS specimen with frequency f_n and amplitude A (cm) will be identified as F[f_n]-A[A]. The LFS specimen with the lowest frequency and amplitude (F2-A1.5) has 25% of its web at approximately zero bending stress, while the rest of the web increases towards 318 MPa at the web extremities (approaching the yield stress). As amplitude increases from 1.5 cm to 3 cm (from F2-A1.5 to F2-A3), more of the web is at zero bending stress, and the maximum stress at the top and bottom of the web decreases. As frequency f_n increases from 2 to 2.5 to 4, these same trends of reduced web participation in bending are observed.

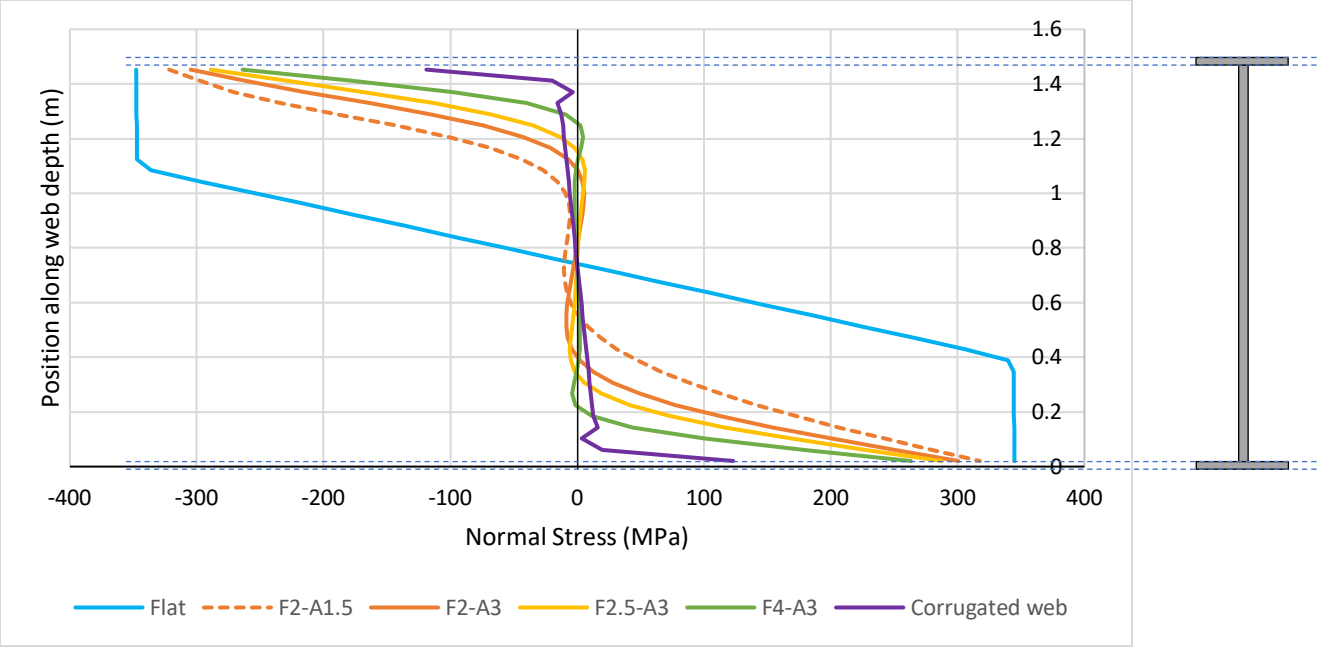

Figure 7. Bending Stress Distribution through the Web Depth, for different LFS specimens shown. In the legend, LFS specimen with frequency f_n and amplitude A (cm) is identified as F[f_n]-A[A].

The bending stress distributions correspond to the maximum moment M_u attained by each specimen for this Set 3a, as listed in Table 3. It is seen that the flat web girder has the highest moment strength due to the high participation of its web in resisting moment. The flat web case achieves an ultimate moment M_u = 6735 kN-m, which is equal to 95% of the plastic moment M_p of the cross section, as shown in the M_u/M_p column of Table 3 (the remaining 5% is due to the center of the web not reaching yield as shown in Fig. 7). The corrugated web girder has the minimum M_u = 4992 kN-m (74% of the flat web M_u), and is very close to the flanges-only Eurocode capacity M_f = 4966 kN-m. The LFS web girders fall between these two moment strengths, with ultimate moment strengths from 76% to 85% of the flat web girder, and with LFS with larger f_n approaching M_f. Essentially, as the amplitude and frequency increase, the ultimate moment capacity decreases (i.e. they are inversely related). Overall, LFS webs experience about a 20% drop in M_u compared to flat webs – they also achieve about 75% of the plastic moment M_p and 5% more moment strength than the flanges-only M_f capacity.

Set 3b of Table 3 shows the maximum shear V_u and moment M_u sustained by the flat, LFS, and corrugated web specimens in the cantilever point loading scenario in Fig. 6. Here the shear V_u is equal to the applied point load P at failure, and M_u is the moment at the cantilever support obtained by the product of $P*a$, where a is the length of the cantilever. It is observed that all three girders fail in flexure (moment capacity). The flat web sustains the largest point load in this scenario because it has the highest moment capacity based on the pure moment study. No reduction in moment capacity due to high shear is observed. The moment at the cantilever support is even slightly higher than the ultimate moment capacities determined for each specimen under pure moment. This is due to observed strain hardening at the cantilever support, similar to Basler's description of strain hardening at the interior supports of continuous girders (Basler 1961). In the strain hardening scenario of cantilever point loading, LFS webs achieve closer to 85% of the plastic moment M_p and 20% more than the flanges-only moment M_f.

Table 3: Larger Span Strength Results for Flat, LFS, and Corrugated Web Girder Specimens.

Set	Loading[1]	Type	Wave Parameters		M_u k-ft (KN-m)	M_u/M_p	M_u/M_f	V_u k (KN)	Failure mode
			f_n	A in. (cm)					
3a	M only	Flat	-	-	4967 (6735)	0.95	1.36	-	Moment
3a	M only	LFS	2	0.59 (1.5)	4197 (5691)	0.81	1.15	-	Moment
3a	M only	LFS	2	1.18 (3)	3987 (5406)	0.77	1.09	-	Moment
3a	M only	LFS	2.5	1.18 (3)	3880 (5261)	0.75	1.06	-	Moment
			4	1.18 (3)	3784 (5130)	0.73	1.03	-	
3a	M only	Corr.	19	0.79 (2)	3682 (4992)	0.71	1.01	-	Moment
3b	V+M (point)	Flat	-	-	5024 (6811)	0.97	1.37	260 (1156)	Moment
3b	V+M (point)	LFS	2.5	1.18 (3)	4411 (5980)	0.85	1.20	228 (1015)	Moment
3b	V+M (point)	Corr.	19	0.79 (2)	4007 (5432)	0.77	1.09	207 (922)	Moment
3b-u	V+M (unif.)	Flat	-	-	4365 (5918)	0.84	1.19	452 (2009)	Shear
3b-u	V+M (unif.)	LFS	2.5	1.18 (3)	4496 (6095)	0.86	1.23	465 (2069)	Moment
3b-u	V+M (unif.)	Corr.	19	0.79 (2)	4018 (5447)	0.77	1.10	416 (1849)	Moment

1. Pure Moment loading (M only) and two different types of High Shear – High Moment (V+M) loading are shown.

In contrast, for the cantilever under a uniformly distributed load, different failure modes are observed. Set 3b-u gives the maximum shear V_u and moment M_u sustained by the flat, LFS, and corrugated web specimens in the cantilever uniform loading scenario shown in Fig. 2(a) and Fig. 6. Here the shear V_u is experienced at the support and equal to the applied load wa at failure, and M_u is the moment at the cantilever support $wa^2/2$, where a is the length of the cantilever (see Fig. 6). Since $P=wa$, the maximum moment for the uniform loading scenario ($Pa/2$) is half the maximum moment experienced by the point loading scenario (Pa). With a smaller ratio of applied shear to moment in the uniform loading case, the LFS web performs better.

For the uniform loading scenario, it is observed that the LFS web and corrugated web reach their moment capacity while the flat web prematurely fails in shear. This is because the shear capacity of the flat web girder is lower compared to the LFS and corrugated webs as indicated previously. Moreover, the LFS web and corrugated webs are able to sustain a greater load wa at the support (roughly twice as high) than in the point-loading case, due to the lower moment associated with the uniform load (see Fig. 6). For the LFS and corrugated webs, the uniform loading M_u values are

16% and 9% higher than the ultimate moment capacities determined under pure moment, due to the strain hardening at the cantilever support. This allows the LFS and corrugated webs to reach 86% and 77% of their cross section's $M_{p,}$ respectively. Just as in the point load scenario, no reduction in moment capacity due to high shear is observed. The LFS web sustains the largest load *wa* in this loading scenario because it has sufficient moment capacity (higher than the corrugated web) and an elevated shear capacity over the flat web. This analysis shows that the LFS web can still be useful in areas of combined shear and moment, though it depends on the ratio of shear-to-moment.

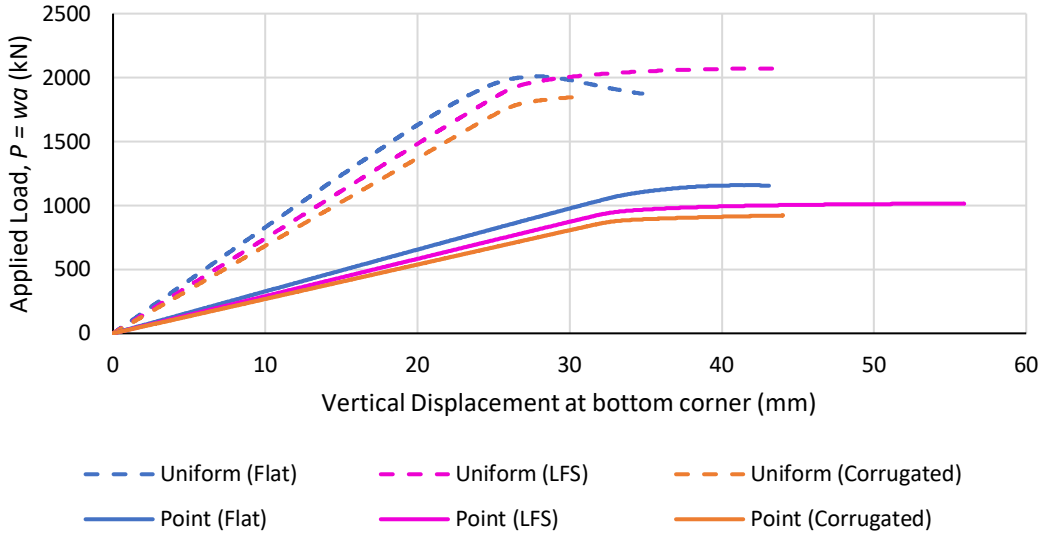

Figure 8: Load displacement curves of cantilever loading scenarios (High shear – high moment)

Fig. 8 shows the load-displacement curves of the 3b and 3b-u Set (cantilever point load and cantilever uniform load, respectively), which permits an evaluation of the stiffness of the flat, LFS, and corrugated specimens. The load applied is either *P* or *wa,* and the displacement is the vertical displacement at the free end of the cantilever. For both loading scenarios, the flat web has the highest vertical stiffness, while the LFS has a reduced stiffness and the corrugated web has the lowest stiffness. The vertical stiffness associated with the point loading is lower than the uniform loading, as expected.

7. Summary and Conclusions

In this paper, plate girders with flat and LFS (low-frequency sinusoidal) webs are studied to determine their combined shear and moment behavior. LFS webs have wavelengths on the order of a meter. The introduction of LFS plates by the authors in a previous study provided an efficient and reliable strategy for increasing the shear strength of thin steel plates by inducing low-frequency sinusoids along the plate's longitudinal axis (Wang et al. 2021). Validated nonlinear finite element models enabled the evaluation of elastic buckling and ultimate strength for several load conditions: pure shear, high shear (*hV*) – small moment (*sM*), pure moment, and high shear (*hV*) – high moment (*hM*) (with point and distributed load). The results of the study are summarized as follows:

- Under pure shear loading conditions, LFS webs with normalized wave frequencies (f_n) values greater than 1.5 can achieve a substantial increase in shear strength when compared to flat webs for both short and long span members.
- The pure moment loading studies show that the LFS webs have a reduced moment capacity, on average about 80% of the flat web. The greater the sinusoidal frequency f_n or amplitude A, the less the web contributes to the section's moment resistance.
- Small moments have little to no effect on the elastic shear buckling load and ultimate shear capacity of LFS webs regardless of f_n value.
- The cantilever stiffness of LFS webs fell between the stiffness of flat and corrugated webs.
- Where high shear and high moment occur under a cantilever with point loading, moment was the controlling failure mode for both LFS and flat webs, with the flat web girder able to sustain 14% more moment than the LFS girder. However, for a cantilever with uniform loading, the LFS girder was able to sustain a 3% larger shear load than the flat web girder (and a 12% higher moment load than the corrugated web girder). Hence, designers may benefit by using LFS webs sections where high shear and high moment occur under a distributed load condition (where ratios of moment to shear are lower than a point load scenario).

In summary, when significant shear strength is needed, LFS plates fabricated correctly with a pure sinusoid can be suitable for sections experiencing high shear and negligible moment. Where the girder is expected to carry significant moment, if the ratios of moment to shear are relatively low, it is possible for an LFS girder to outperform a flat web girder. However, where the moment to shear ratios are large, the flanges should be enhanced since the LFS web has a reduced capacity for carrying bending moment loads. This study shows the potential applications of LFS and encourages a more in-depth examination of moment-shear interaction in LFS plate girders, including the effects of lateral torsional buckling (LTB), where preliminary results show LFS plate girders can have larger LTB resistance over flat webs.

Nomenclature

A_f = area of one flange;
A_w = web area;
a = longitudinal panel length;
CP = cantilever panel;
D = web depth;
FB = full beam;
F_y = yield stress;
H = distance between flange centroids;
hM = high moment;
hV = high shear;
LFS = low-frequency sinusoids;
MP = moment panel;
M_f = flange moment;
M_p = plastic moment;
M_u = maximum (ultimate) moment capacity;
sM = small moment;

sV = small shear;
V_{cr} = elastic shear buckling load;
V_p = plastic shear strength;
V_u = ultimate shear strength.

Acknowledgments
This research was sponsored by the National Science Foundation (NSF) under grants CMMI-1662886 and CMMI-1662964. All opinions expressed in this paper are the authors' and do not necessarily reflect the policies and views of the sponsors. The authors would like to acknowledge Ted P. Zoli for his consultation and conceptualization in this work.

References

Abbas, H.H., Sause, R., Driver, R.G. (2006). "Behavior of Corrugated Web I-Girders under In-Plane Loads." *Journal of Engineering Mechanics,* 132 (8) 806-814.

Azizinamini, A., Hash, J.B., Yakel, A.J., Farimani, R. (2007). "Shear Capacity of Hybrid Plate Girders." *Journal of Bridge Engineering,* 12 (5) 535–43. https://doi.org/10.1061/(asce)1084-0702(2007)12:5(535).

Balaji Rao, K.., Anoop, M.B., Raghava, G., Prakash, M., Rajadurai, A. (2013). "Probabilistic Fatigue Life Analysis of Welded Steel Plate Railway Bridge Girders Using S-N Curve Approach." *Proceedings of the Institution of Mechanical Engineers, Part O: Journal of Risk and Reliability,* 227 (4) 385–404. https://doi.org/10.1177/1748006X13480754.

Basler, K., Thurlimann, B. (1961). "Strength of Plate Girders in Bending." Welded Plate Girders Report No. 251-19. Lehigh University, Bethlehem, PA.

Basler, K, Yen, B.T., Mueller, J.A., Thurlimann, B. (1960). "Web Buckling Tests On Welded Plate Girders." Lehigh University, Bethlehem, PA.

Basler, Konrad. (1961). "Strength of Plate Girders under Combined Bending and Shear." *Journal of Structural Engineering, ASCE* 87: 181–97. http://preserve.lehigh.edu/engr-civil-environmental-fritz-lab-reports/71.

CEN. (2001). Eurocode 3: Design of steel structures: Part 1.2 General rules - Structural fire design. London: BSI.

CEN. (2006). "Part 1-5: Plated structural elements. Annex D (informative)- Plate girders with corrugated webs." In EN 1993-1-5 (2006) (English): Eurocode 3: Design of steel structures, 45-52. Brussels.

Dassault Systemes. (2017). "Abaqus 2017 Documentation." *User's Manual, Version 6.17. Dessault Systémes, Simulia Corp.,* Providence, RI.

Driver, R.G, Abbas, H.H., Sause, R. (2006). "Shear Behavior of Corrugated Web Bridge Girders." *Journal of Structural Engineering, ASCE* 132 (2) 195–203. https://doi.org/10.1061/ASCE0733-94452006132:2195.

FHWA. (1982). "Volume II, Structural Steel Superstructures." In *Standard Plans for Highway Bridges*.

Glassman, J.D., Garlock, M.E.M. (2016). "A Compression Model for Ultimate Postbuckling Shear Strength." *Thin-Walled Structures,* 102 258–72. https://doi.org/10.1016/j.tws.2016.01.016.

Gomez, A. 2020. "Web Out-of-Straightness in Plate Girders: Methodology for Measure- Ments and Effects on Shear Capacity." Princeton University.

Graciano, C., Ayestarán, A. (2013). "Steel Plate Girder Webs under Combined Patch Loading, Bending and Shear." *Journal of Constructional Steel Research,* 80 202–12.

Grubb, M.A., Schmidt, R.P. (2012). "Design Example 1: Three-Span Continuous Straight Composite Steel I-Girder Bridge." In *Steel Bridge Design Handbook FHWA-IF-12-052 Vol 20*. FHWA.

Lee, S.C., Davidson, J. S., Yoo, C. H. (1996). "Shear Buckling Coefficients of Plate Girder Web Panels." *Computers and Structures,* 59 (5) 789–95. https://doi.org/10.1016/0045-7949(95)00325-8.

Lee, S.C., Lee, D.S., Yoo, C.H. (2013). "Flexure and Shear Interaction in Steel I-Girders." *Journal of Structural Engineering (United States),* 139 (11) 1882–94. https://doi.org/10.1061/(ASCE)ST.1943-541X.0000746.

Pasternak, H., Kubieniec, G. (2010). "Plate Girders with Corrugated Webs." *Journal of Civil Engineering and Management,* 16 (2) 166–71. https://doi.org/10.3846/jcem.2010.17.

Riahi, F., Behravesh, A., Yousefzadeh Fard, M., Armaghani, A. (2018). "Shear Buckling Analysis of Steel Flat and Corrugated Web I-Girders." *KSCE Journal of Civil Engineering,* 22 (12) 5058–73. https://doi.org/10.1007/s12205-017-1530-9.

Sayed-Ahmed, E.Y. (1998). "Corrugated Steel Web Plate / Box Girders: Bridges of the 21st Century."

Siokola, W. (1997). "Corrugated web beam - production and application of girders with corrugated web." *Der Stahlbau,* 66 (9) 595-605.

Škaloud, M., Zörnerová, M., Urushadze, S. (2013). "Breathing-Induced Fatigue in Thin-Walled Construction." *Procedia Engineering,* 66 (ii): 383–92. https://doi.org/10.1016/j.proeng.2013.12.092.

Timoshenko, S.P., Gere, J.M. (1960). *Theory of Elastic Stability, Second Edition.* McGraw-Hill Book Company Inc, New York, NY.

Wang, P.Y., Garlock, M.E.M., Zoli, T.P., Quiel, S.E. (2021). "Low-Frequency Sinusoids for Enhanced Shear Buckling Performance of Thin Plates." *Journal of Constructional Steel Research,* 177 1–11. https://doi.org/10.1016/j.jcsr.2020.106475.

Wang, P.Y, Garlock, M.E.M., Medlock, R., Zoli, T.P., Quiel, S.E. (2020). "Low-Frequency Sinusoidal Web Girders Using Conventional Fabrication Techniques," *IBC Proceedings 2020.*

Wang, P., Augustyn, K., Gomez, A., Quiel, S.E., Garlock, M.E.M. (2019). "Influence of boundary conditions on the shear post-buckling behavior of thin web plates." *Conference Proceedings of the 2019 SSRC Annual Stability Conference.* St. Louis, MO

White, D.W., Barker, M.G. (2008). "Shear Resistance of Transversely Stiffened Steel I-Girders." *Journal of Structural Engineering,* 134 (9) 1425–36. https://doi.org/10.1061/(asce)0733-9445(2008)134:9(1425).

White, D.W., Barker, M.G., Azizinamini, A. (2004). "Shear Strength and Moment-Shear Interaction in Transversely-Stiffened Steel I- Girders." *Structural Engineering, Mechanics and Material,* 27.